# AUTOMATED SENSOR ORIENTATION ESTABLISHMENT FOR HIGH RESOLUTION SATELLITE IMAGES BY IMPROVED GCP CHIP MATCHING

Hyeon-Gyeong Choi[1], Sunghyeon Kim[2] and Taejung Kim*[3]
[1]Graduate Student, [2]Undergraduate Student, [3]Professor
Dept. of Geoinformatic Engineering, Inha University
100 Inha-ro, Michuhol-gu, Incheon 22212, Republic of Korea
Email: hkChoi@inha.edu, 12181204@inha.edu, tezid@inha.ac.kr*

**KEY WORDS:** Sensor orientation, Geometric correction, GCP matching, High-resolution satellite, Mid-resolution satellite

**ABSTRACT:** Correcting geometric distortions in satellite images is crucial for their effective utilization. Geometric distortion correction is performed by establishing a precise sensor orientation. Automated precision sensor orientation is essential for the rapid delivery of satellite images. For this, one of the key processes is GCP (Ground Control Point) chip matching. Our previous research developed a method of GCP chip matching at sub-pixel scale of satellite images and achieved a sub-pixel accuracy for mid-resolution images. In this paper, we enhance our previous method further with high-resolution satellite images and to achieve precise geometric accuracy automatically. Our method begins by establishing an initial sensor model using rational polynomial coefficients (RPC) provided with the original satellite image. The initial model is then used to search for all GCP chips within the boundaries of the satellite image. Next, we define areas surrounding each GCP chip and resampled GCP chips and satellite images according to desired match scale. Then, we apply GCP chip matching from coarse scale to finer scale up to desired sub-pixel level. Finally, we establish a precision sensor orientation based on the matching results and verify the accuracy of the sensor model. We tested this method using RapidEye images with a resolution of 5m and Kompsat3A with a resolution of 0.5m. We used GCP chips with 0.25m ground sampling distances. We applied GCP chip matching, up to a desired sub-pixel level. As a result of the study, it was possible to reduce the position error of more than 0.5 pixel in mid-resolution satellite images, and about 0.5 pixel in high-resolution satellite images. This study showed that performing GCP chip matching up to enhanced resolution by upsampling both chips and satellite images could establish a better performance than performing GCP chip matching up to the original resolution. The results of this study are expected to contribute to the improvement of precision sensor orientation performance of satellite images with various GSDs.

## 1. INTRODUCTION

High resolution satellite imagery has gained significant attention and has been extensively utilized in various fields. Accordingly, research is required on how to precisely correct geometric distortion of high-resolution satellite images. According to the CEOS Analysis Ready Data for Land (CARD4L), the certification criterion for geometric accuracy is known to achieve an accuracy of rRMSE 0.5pixels. (Boccia *et al.*, 2021) Correcting geometric distortions in satellite images is crucial for their effective utilization. Geometric distortion correction is performed by establishing a precise sensor orientation. Automated precision sensor orientation is essential for the rapid delivery of satellite images. For this, one of the key processes is GCP (Ground Control Point) chip matching. GCP chip refers to an image segment in which the coordinates of its center are accurately known. A technology has been developed that was able to automatically extract GCPs by performing matching between GCP coordinates and image coordinates of satellite images using this image segment. (Son *et al.*, 2021)

In order to automatically establish a precise sensor orientation, research has been conducted to improve the matching performance of satellite images and GCP chips. In the study by Shin *et al.*, they conducted chip matching experiments using pan-sharpening images to establish precision sensors orientation for high-resolution satellite images. (Shin *et al.*, 2018) Pan-sharpening is a process of merging high-resolution panchromatic and lower resolution multispectral imagery to create a single high-resolution color image. It was found that performance improved when performing GCP chip matching using pan-sharpened images rather than using the original multispectral image. In the study by Lee and Kim, they used satellite image upsampling instead of pan-sharpening to improve the matching performance in mid-resolution satellite images without panchromatic band. (Lee and Kim, 2021) It showed that the results of matching by applying upsampling had better performance in geometric accuracy than performing matching in the original resolution.

Previous studies indicate that the spatial resolution of GCP chips and satellite images was related to sensor model performance. In this study, we apply improved upsampling to establish a more precise sensor orientation for mid-resolution and high-resolution satellite images. Since we use GCP chip database with very high resolution, there is a significant difference in resolution among the GCP chips and mid-resolution satellite images. In contrast, there is only a slight difference in resolution among GCP chips and high-resolution satellite images. Therefore, when upsampling a high-resolution satellite image, we propose a new GCP chip matching by applying upsampling to both GCP chips and satellite images at the same time. Through this study, we would like to find out the effectiveness of the method of matching the GCP chip on the sub-pixel scale of satellite images when establishing a precision sensor orientation.

## 2. MATERIALS AND METHODS

In this study, we used GCP chips as shown in Figure 1. Table 1 describes information of GCP chips we used.

Figure 1. Example of GCP Chip (Left: South Korea, Right: North Korea).

| Area | South Korea | North Korea |
|---|---|---|
| Ground coordinates reference | Unified control point, Triangulation point, Photo control point | Plane coordinates of orthogonal image & DEM Ellipsoidal Height |
| Raw data | Aerial photography (Orthophoto) | Satellite ortho image |
| Chip size (pixel) | 1027×1027 | 513×513 |
| Resolution | 0.25 m | 0.50 m |
| Band | Red, Green, Blue | Gray |

Table 1. Specifications for GCP Chip used.

In this study, we used mid-resolution satellite images as shown in Figure 2. Table 2 describes their information.

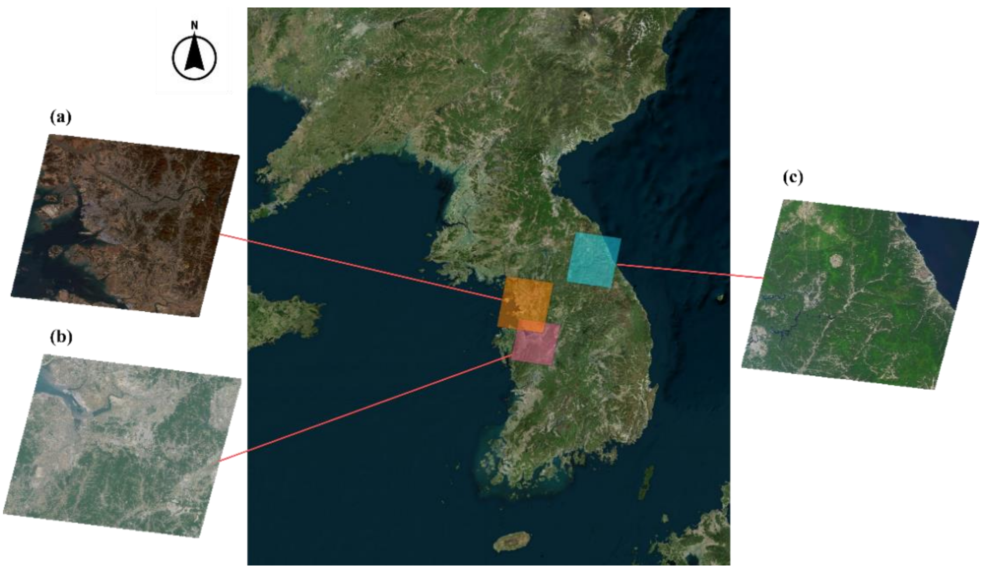


Figure 2. Used data as mid-resolution satellite images(Area).
(a): Incheon, (b): Cheonan, (c): Yanggu

| ID | (a) | (b) | (c) |
|---|---|---|---|
| **Area** | Incheon | Cheonan | Yanggu |
| **Satellite image** | RapidEye L1B | | |
| **Spectral resolution** | Blue(440~510nm)<br>Green(520~590nm)<br>Red(630~685nm)<br>RedEdge(690~730nm)<br>NIR(760~850nm) | | |
| **Pixel size** | 5 m | | |
| **Acquisition date** | 2019. 11. 07 | 2019. 06. 04 | 2019. 05. 24 |
| **Image size (pixel)** | 11824×14509 | 11754×11965 | 11760×14196 |
| **Quantity of GCP chip** | 1830 | 1304 | 1604 |

Table 2. Specifications for mid-resolution satellite images used.

In this study, we used high-resolution satellite images as shown in Figure 3. Table 3 describes their information.

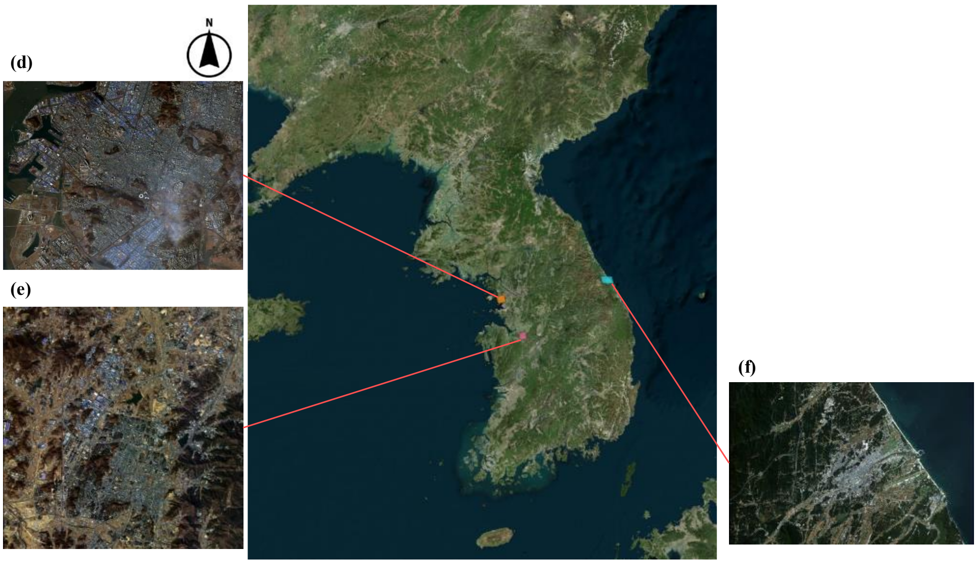


Figure 3. Used data as high-resolution satellite images(Area).
(d): Incheon, (e): Cheonan, (f): Gangneung

| ID | (d) | (e) | (f) |
|---|---|---|---|
| **Area** | Incheon | Cheonan | Gangneung |
| **Satellite image** | Kompsat3A L1R | | |
| **Spectral resolution** | Panchromatic<br>(450~900nm)<br><br>Multispectral<br>Blue(450~520nm)<br>Green(520~600nm)<br>Red(630~690nm)<br>NIR(760~900nm) | | |
| **Pixel size** | Pan: 0.5 m, MS: 2 m | | |
| **Acquisition date** | 2018. 01. 19 | 2019. 01. 29 | 2019. 10. 16 |
| **Image size of Pan (pixel)** | 24060×19080 | 24060×24400 | 24060×16000 |
| **Quantity of GCP chip** | 59 | 55 | 95 |

Table 3. Specifications for high-resolution satellite images used.

We selected the study data as a place with various topographical features. First, Cheonan is mainly distributed in urban areas. In the case of Incheon, the sea is located in the west, so the corrected land part is concentrated to the right of the image. In the case of Gangneung and Yanggu, it is also data that includes the sea, but also includes mountainous areas.

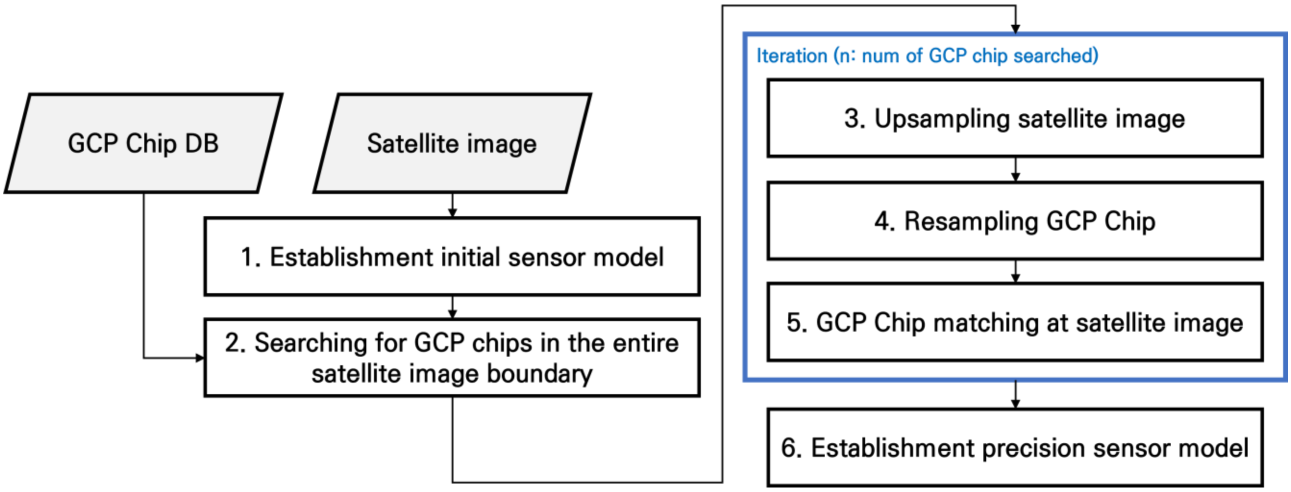

Figure 4. flowchart of the proposed method.

Figure 4 is the flowchart of the proposed method in this study. The proposed method begins by establishing an initial sensor model using rational polynomial coefficients (RPC) provided with the original satellite image. In the case of a high-resolution satellite image with a panchromatic band, we first create a high-resolution color image through pan-sharpening and then use the RPC of the panchromatic band. RPC refers to a coefficient for constructing a sensor model using Rational Function Model (RFM). Equation (1) and (2) is the formulas of RFM according to columns and rows of image, where a, b, c, and d are each RPC.

$$c_n = \frac{P_1(X_n,\ Y_n,\ Z_n)}{P_2(X_n,\ Y_n,\ Z_n)} = \frac{\sum_{i=0}^{3}\sum_{j=0}^{3}\sum_{k=0}^{3} a_{ijk} X_n^i Y_n^j Z_n^k}{\sum_{i=0}^{3}\sum_{j=0}^{3}\sum_{k=0}^{3} b_{ijk} X_n^i Y_n^j Z_n^k} \quad (1)$$

$$r_n = \frac{P_3(X_n,\ Y_n,\ Z_n)}{P_4(X_n,\ Y_n,\ Z_n)} = \frac{\sum_{i=0}^{3}\sum_{j=0}^{3}\sum_{k=0}^{3} c_{ijk} X_n^i Y_n^j Z_n^k}{\sum_{i=0}^{3}\sum_{j=0}^{3}\sum_{k=0}^{3} d_{ijk} X_n^i Y_n^j Z_n^k} \quad (2)$$

This sensor model is then used to search for all GCP chips within the boundaries of the satellite image. Next, we define areas surrounding each GCP chip and upsample satellite image to the desired scale. In this study, we apply an upsampling ratio to each experimental data from 1 to 5 times. Figure 5 shows a high-resolution satellite image to which upsampling ratios 1 to 3 are applied.

Figure 5. GCP chip GSD according to upsampling ratio.
(a): ratio 1 (0.5m), (b): ratio 2 (0.25m), (c): ratio 3 (0.167m)

We resample the GCP chip according to the geometry and adjusted resolution of the satellite image. We use an area-based image matching algorithm for automatic matching, so the process of matching the GCP chip to the resolution and geometry of the satellite image is important. Figure 6 shows the process of resampling the GCP chip according to the geometry and resolution of the satellite image. This process is performed on all GCP chips searched.

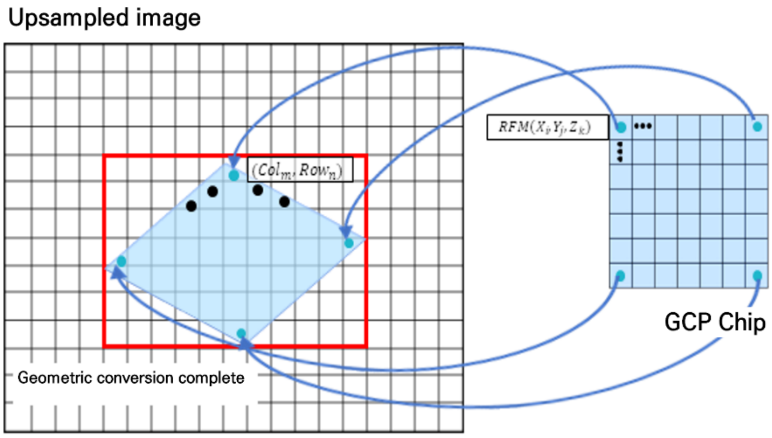


Figure 6. Concept of resampling GCP chip.

Then, we apply GCP chip matching from coarse scale to finer scale up to desired sub-pixel level. In this matching process, we organize and proceed with a pyramid image of four steps to improve the processing speed. We perform image matching from the top layer of the configured pyramid, applying the Census algorithm in the last layer, and applying the ZNCC algorithm in the rest of the layers except for the last layer. Among the automatically matched GCPs, there are inevitably incorrect matching points. We automatically remove them using the RANSAC (Random Sample Consensus) technique. Finally, we establish a precision sensor orientation based on the matching results. In order to establish a precision sensor model, the coefficient of the error correction equation for error correction of the initial sensor model is estimated. The error correction equation is Equation (3), (4).

$$c = a_{11}c_0 + a_{12}r_0 + a_{13} \tag{3}$$

$$r = a_{21}r_0 + a_{22}r_0 + a_{23} \tag{4}$$

In the above formula, $c_o, r_o$ and $c, r$ are image coordinates before and after correction, respectively, and $a_{11} \sim a_{23}$ correspond to the coefficient of the error correction formula. When the coefficient estimation of the error correction equation is completed, we calculate the RPC coefficient again using the error correction equation to establish a precise sensor model. When a precision sensor model is established for each upsampling ratios, we perform the work to convert it back into a precision sensor model of the original resolution for accuracy comparison. We compare the accuracy of the precision sensor model established for each upsampling ratios.

## 3. RESULTS AND DISCUSSION

In this study, we performed accuracy verification at the original resolution and used the model accuracy, check accuracy, and matching success rate as performance evaluation indicators. Model accuracy is the rRMSE measured for the GCP used in the initial sensor model calibration. Check accuracy is rRMSE measured for manual extraction reference points not included in model points. Equation (5) is formula of rRMSE.

$$rRMSE = \sqrt{(RMSE_{col})^2 + (RMSE_{row})^2} \tag{5}$$

| | Model Accuracy (pixel) | | | Check Accuracy (pixel) | | |
|---|---|---|---|---|---|---|
| | Incheon | Cheonan | Yanggu | Incheon | Cheonan | Yanggu |
| 5m | 1.285 | 1.272 | 1.351 | 1.205 | 1.144 | 0.968 |
| 2.5m | 0.626 | 0.608 | 0.632 | 0.766 | 0.422 | 0.928 |
| 1.67m | 0.317 | 0.354 | 0.310 | 0.859 | 0.466 | 0.952 |
| 1.25m | 0.243 | 0.241 | 0.207 | 0.882 | 0.598 | 1.014 |
| 1m | 0.199 | 0.204 | 0.188 | 0.892 | 0.561 | 1.101 |

Table 4. Result of mid-resolution satellite images

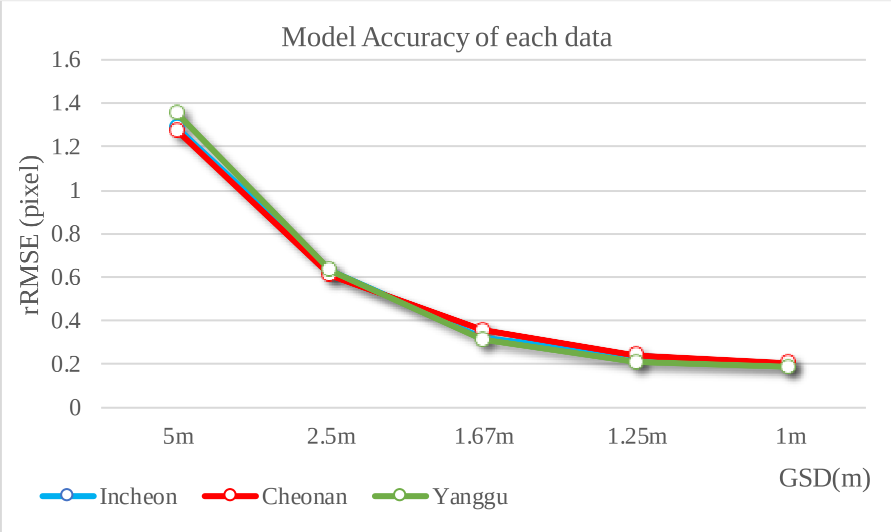


Figure 7. Model accuracy of each data of mid-resolution satellite images.

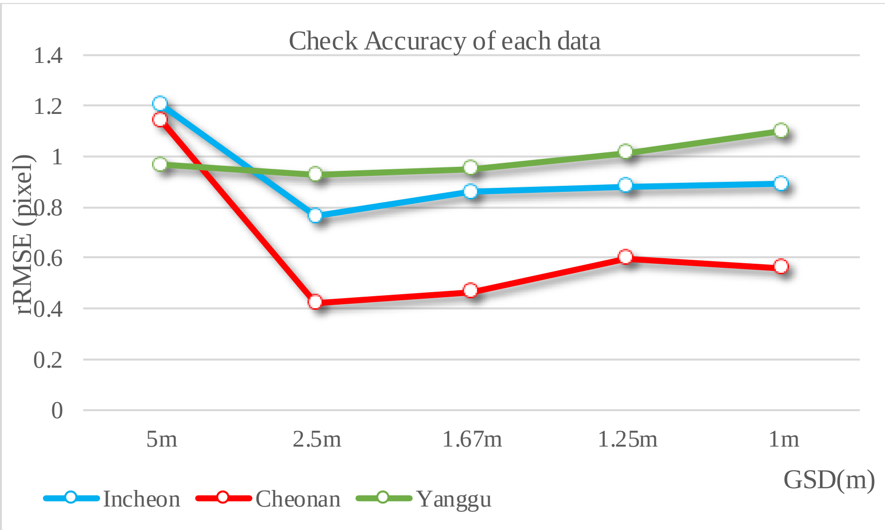


Figure 8. Check accuracy of each data of mid-resolution satellite images.

| | Model Accuracy (pixel) | | | Check Accuracy (pixel) | | |
|---|---|---|---|---|---|---|
| | Incheon | Cheonan | Gangneung | Incheon | Cheonan | Gangneung |
| 5m | 1.43 | 1.154 | 1.376 | 4.114 | 3.108 | 1.979 |
| 2.5m | 0.663 | 0.669 | 0.625 | 3.013 | 0.83 | 1.274 |
| 1.67m | 0.449 | 0.397 | 0.447 | 2.832 | 2.153 | 0.996 |
| 1.25m | 0.31 | 0.363 | 0.309 | 2.96 | 1.385 | 1.306 |
| 1m | 0.29 | 0.266 | 0.275 | 2.39 | 1.577 | 1.36 |

Table 5. Result of high-resolution satellite images

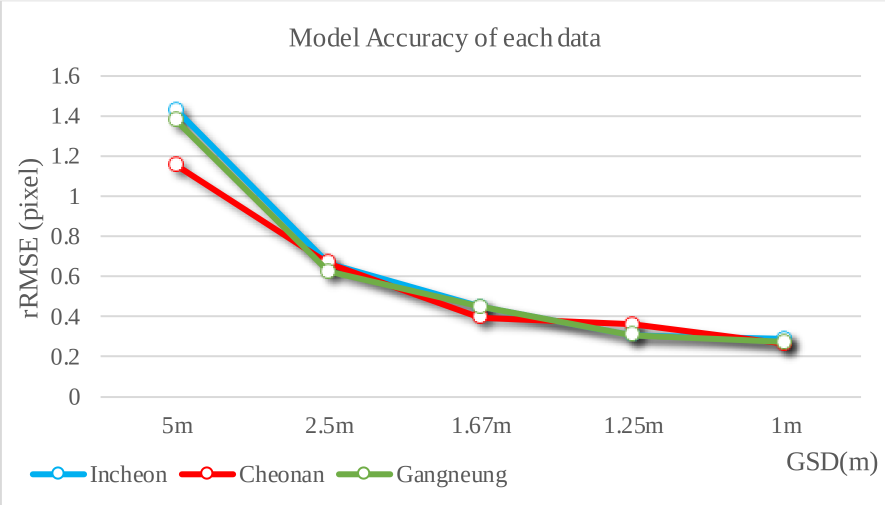


Figure 9. Model accuracy of each data of high-resolution satellite images.

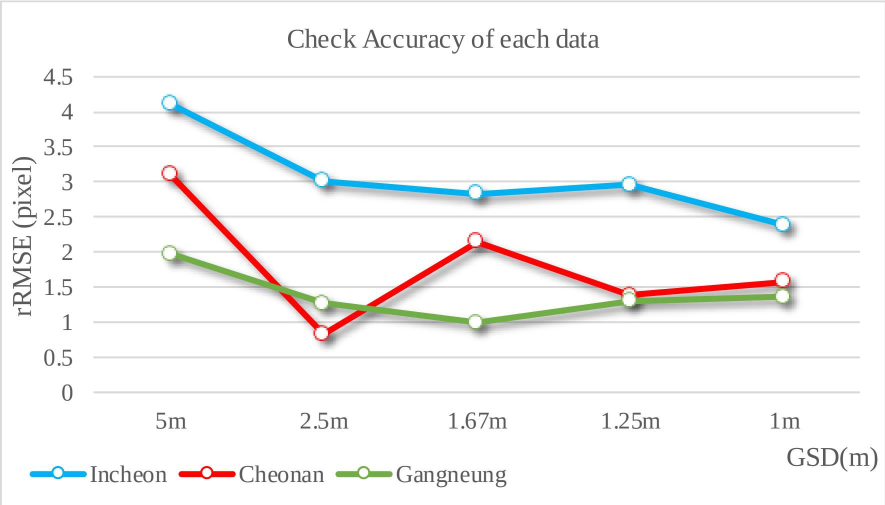


Figure 10. Check accuracy of each data of high-resolution satellite images.

Table 4 is a table showing the experimental results on mid-resolution satellite images. Table 5 is a table showing the experimental results on high-resolution satellite images. Figure 7 and 9 show that model accuracy was improved with higher upsampling ratios and smaller GSDs. This indicates that estimation process for RPC updates was applied successfully. Figures 8 and 10 show that check accuracy was improved with higher upsampling ratios and smaller GSDs. This indicates that the matching performance at the resolution applied with upsampling improved more than the matching performance at the original resolution. However, topographical factors seemed to affect matching performance. In the case of Yanggu area in mid-resolution satellite images, there are many mountainous areas. Accordingly, we thought that unclear matching points would have affected the model's establishment.

## 4. CONCLUSION

This study proposed a method of matching GCP Chip at the sub-pixel scale of satellite images through satellite image upsampling when establishing a precision sensor orientation for mid-resolution and high-resolution satellite images. As a result of the experiment, we confirmed that the matching performance improved when upsampling was applied to both mid-resolution and high-resolution satellite images. Among the results of experiments using mid-resolution satellite images, there were cases where the check accuracy was close to 0.5 pixels or less than 0.5 pixels. This means that the CARD4L geometric accuracy criteria, which were difficult to achieve when establishing sensor orientation at the original resolution, are likely to be achieved through satellite image upsampling. In the experiment using high-resolution satellite images, we upsampled satellite images and chip images simultaneously. As a result of the experiment, we confirmed that a more precise sensor orientation was established in upsampled matching than in the matching at the original resolution. This indicates the possibility of reducing geometric errors through high-resolution satellite image through upsampled matching. This may also indicate the need of GCP chips at very high resolution for further accuracy improvement. Therefore, further research is needed to improve the performance of establishing a high-resolution satellite image precision sensor orientation. It is also necessary to consider using ultra-high-resolution data such as drones. It is hoped that the results obtained through this study can be helpful in image processing and utilization of satellite images.

**ACKNOWLEDGEMENTS**

This work was carried out with the support of "Cooperative Research Program for Agriculture Science and Technology Development (Project No. PJ 016233)" Rural Development Administration, Republic of Korea.

**REFERENCES**

Boccia, V., R.Q. Iannone, and F. Gascon, 2021. Copernicus Sentinel-2 Data From A Card4L Perspective: Preliminary Self-Assessment Performed by Esa. In: *IEEE International Symposium on Geoscience and Remote Sensing*, Brussels, Belgium, pp. 1994-1996.

Lee, Y. and T. Kim, 2021. Determination of Spatial Resolution to Improve GCP Chip Matching Performance for CAS-4. *Korean Journal of Remote Sensing*, 37(6-1), pp. 1517-1526.

Shin, J.I., T. Kim, W.S. Yoon, and H.J. Park, 2018. Improving Satellite-Aerial Image Matching Success Rate by Image Fusion. In: *European Conference on Electrical Engineering and Computer Science*, Bern, Switzerland, pp. 224-227.

Son, J.H., W. Yoon, T. Kim, and S. Rhee, 2021. Iterative Precision Geometric Correction for High-Resolution Satellite Images. *Korean Journal of Remote Sensing*, 37(3), pp. 431-447.